Neuro-Fuzzy Hybrid System Applied to the Optimal Reactive Power Flow Problem

MAURY MEIRELLES GOUVÊA JR.[1] LUIZ DANILO BARBOSA TERRA[2]
[1]Faculty of Pedro Leopoldo
R. Teófilo Calazans de Barros 100, 33.600-000, Pedro Leopoldo, MG
[2]Pontifical Catholic University of Minas Gerais
Av. Dom Jose Gaspar 500, 30.535-610, Belo Horizonte, MG
BRAZIL

Abstract: - In this paper, the integration of Artificial Intelligence and sensitivity analysis is described for the formulation and resolution of the optimal reactive load flow problem. Instead of formulating of a scalar optimization problem, the development of a fuzzy multi-objective programming is proposed. This treatment considers all the objectives and constraints in a satisfaction degree. Additionally, an Artificial Neural Network is used to supply the voltage collapse margin of the weakest bus, also considered an additional objective in the problem. The several steps and advantages involving this approach applied to the multi-objective problem are discussed. The developed algorithm makes it possible to create a fuzzy decision function that can optimize the reactive power flow, while eliminating voltage violations. The efficiency of the method is investigated in case studies using the standard IEEE-30 bus bar system.

Key-Words: - Optimal Reactive Power Flow; Fuzzy Sets; Fuzzy Programming; Multi-criteria Optimization; Artificial Neural Network; Non Linear Programming.

1 Introduction

The Optimal Reactive Power Flow (ORPF) problem has concentrated attention in recent researches because of the increase in energy demand each year, as well as financial and ambient constraints. An adequate reactive power planning must guarantee the conditions for an economic and secure operation of the power systems in the base case and all contingencies.

In many cases, the ORPF problem is treated as a one objective constrained optimization problem. Nevertheless, frequently many objectives, as the active power loss, the generator reactive power reserve, the voltage profile and the stability index are to be accounted for simultaneously in the ORPF problem solution. When only one of those objectives is accounted for, the solution is relatively simple and fast; but, if many objectives are to be considered, the solution becomes more complicated because the optimums points may not be coinciding. The solution is to find out a compromise solution point which satisfy all objectives.

There are many methods which treat the multiobjective problem. In parametric solution [1], the objectives are weighted by coefficients that determine their relative relevance. In the ε-constraint approach [1], only the most important objective is accounted for and the others are replace as constraints. In the last years, Artificial Intelligence (AI) techniques have been used to provide multi-objective problem solutions. Mohandas et al. applied the fuzzy set theory [2] to weight the many objectives in the structural optimization problem [3]. Ramesh and Li utilized a fuzzy multi-objective approach to ORPF problem solution [4]. The Artificial Neural Networks (ANN's) technology has been researched and applied in control, identification, recognition theories and others [5]. Specifically in Power Systems, the ANN's have been utilized in security assessment [6], fault diagnose [7] and load forecast [8].

This work presents a new methodology to solution the ORPF problem. The problem is formulated as a non-linear multi-objective problem which integrates the sensitive analysis of power systems with two AI Techniques – the fuzzy sets and ANN's. The function of the ANN is to yield the voltage collapse margin (VCM) of the weakest bus, in the voltage viewpoint, and to influence the control actions along the optimization process. The objectives, conforming and conflicting, are treated by satisfaction degrees weighted by linguistic terms. The objective functions are replaced by a pertinence function weighted by sum which describes the satisfaction of all objectives. The objective of this approach is to find out a correct numeric weight which yields the optimal solution. The method is evaluated in case study in IEEE-30 bus bar systems. The effects and advantages of the improvement in a VCM of the system are investigated varying important parameters of the optimization process.

2 Artificial Neural Networks

2.1 Artificial Neural Networks Topology

The Artificial Neural Networks (ANN's) are an analogy of biology neural networks, simulating its comportment in digital computer or hardware board. There are many models of ANN's, used in concordance with applications. In this work, the feedforward model, introduced in 1958 by Rosenblatt [9], is used. The feedforward model is an artificial neurons set massively joined, organized in layers, as show in Figure 1. The signals are applied from input layer to output layer, passing per each layer.

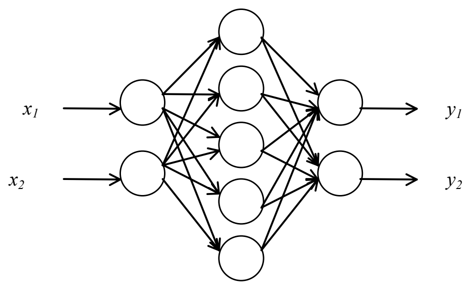

Fig. 1: Feedforward Network Model

The signals, arrived in each neuron, are weighted by coefficients, called synaptic weight, and summed in the body of the main neuron. The neuron output is defined by a non-linear function and activated if the weighted sum of the output is greater than bias value; if not, the output is not activated. Thus, the output neuron is defined by

$$y = f(v) \tag{1}$$

where

$$v=\sum_{i=1}^{n} W_i \; x_i \; - \; \theta \tag{2}$$

where W_i is the synaptic weight, x_i is the neuron input and θ is the bias of the neuron.

2.2 Artificial Neural Networks Training

The ANN is strongly applied after Rumelhart et al [10] introduced Backpropagation algorithms training. The ANN training, or ANN learning, is performed by environment examples (patterns set) represented by input/output pair. In the learning process, the ANN adapts itself adjusting their synaptic weight to produce a performance which it is projected. The patterns set is defined by

$$\psi = \{(X_l \, , Y_l^d)\}_{l=1}^{P} \tag{3}$$

where $(X_l \, , Y_l^d)$ is l-th pattern, X_l^d is the l-th input vector and Y_l^d is the l-th desired output vector. In the ANN training, a signal is applied and one output signal is obtained; if this output is different of Y_l^d there is an error and the synaptic weight must be adjusted. The Backpropagation algorithm treat the training as a non constrained global optimization problem, where the quadratic error function, to be minimized, is defined by

$$E_p = \frac{1}{2} \sum_{i=1}^{m} (y_i^d - y_i)^2 \tag{4}$$

where m is the number of ANN output. The patterns are presented sequentially until existing difference between the ANN output and the desired output, considering all P patterns, is greater than ε tolerance. The adjust of j-th weight of the i-th neuron is defined by

$$\Delta W_{ij} = -\eta \, \delta_i \, x_j \tag{5}$$

where

$$\delta_i = -(y_i^d - y_i) \; f'(v_i) \tag{6}$$

for output layer and

$$\delta_i = f'(v_i) \sum_{j=1}^{m} \delta_j \, \frac{\partial v_j}{\partial y_i} \tag{7}$$

for hidden layer. The η coefficient, called learning tax, determine the step length under the quadratic error function surface.

3 Multi-Objective Fuzzy Programming Applied to the ORPF

3.1 Multi-objective Fuzzy Programming Basic

The Linear Programming (LP) with two objectives can be stated as:

$$Max \;\; Z = C \, X \tag{8}$$

subject to

$$AX \le b \quad (9)$$

$$X \ge 0 \quad (10)$$

where X is the vector of the n decision variables, C is a individual costs matrix of X with respect to Z, b is the vector of the m constraints of the system and A is the sensitivity matrix of dimension m x n. Equation (8) can also be wrote as

$$Max \quad Z = \begin{bmatrix} c_{11} & c_{12} \\ c_{21} & c_{22} \end{bmatrix} \begin{bmatrix} x_1 \\ x_2 \end{bmatrix} \quad (11)$$

Separating Z function into two distinct objectives $Z_1 = c_{11}x_1 + c_{12}x_2$ and $Z_2 = c_{21}x_1 + c_{22}x_2$, trough the graphical solution of Figure 2, optimum values for x_1 and x_2 with respect to Z_1 do not correspond to the optimum values for Z_2, and vice versa. The feasible solution region is limited by five constraints and for the straight lines r and s, which represent the maximum values for the objectives Z_1 e Z_2 respectively.

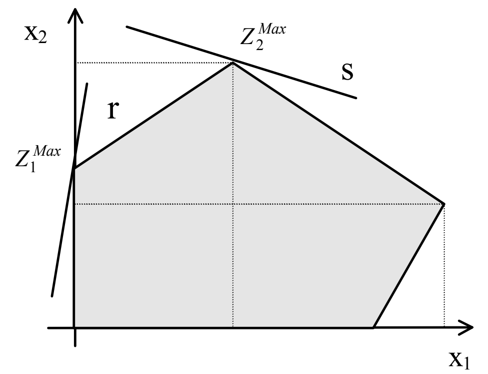

Fig. 2: Set of feasible solutions for an LP problem

In Fuzzy Goal Programming [3], the objectives and constraints are associated with fuzzy sets, represented by membership functions, which determine their satisfactions. The membership functions of the problem (8)-(10), with respect to Fuzzy Goal Programming, are described as

$$\mu_{g1} = \begin{cases} 1 & \text{for } Z_1 = Maximum \quad Value \ 1 \\ \mu_1(Z_1) & \text{for } Z_1 < Maximum \quad Value \ 1 \end{cases} \quad (12)$$

$$\mu_{g2} = \begin{cases} 1 & for \ Z_2 = Maximum \quad Value \ 2 \\ \mu_2(Z_2) & for \ Z_2 < MaximumVal \quad ue \ 2 \end{cases} \quad (13)$$

$$\mu_{gi} = \begin{cases} 1 & for \ \mathrm{a_{i1}x_1 + a_{i2}x_2 \le b_i} \\ \mu_i(Ax) & for \ \mathrm{a_{i1}x_1 + a_{i2}x_2 > b_i} \end{cases}, for \ i = 1, \cdots, m \quad (14)$$

$$\mu_{gj} = \begin{cases} \mu_j(x) & \mathrm{x_j} < 0 \\ 1 & for \ \mathrm{x_j} \ge 0 \end{cases}, for \ j = 1, \cdots, n \quad (15)$$

where, μ_{gk} is the membership function for the objective k, which describes the corresponding fuzzy set.

For the resolution of problem (8)-(10) the objective function is formed by the weighted sum of all objectives. The weigh is realized by fuzzy sets, using linguistic terms, such as *"high_weight"*, *"medium_weight"* and *"low_weight"*. Figure 3 shows the fuzzy sets with the linguist weights.

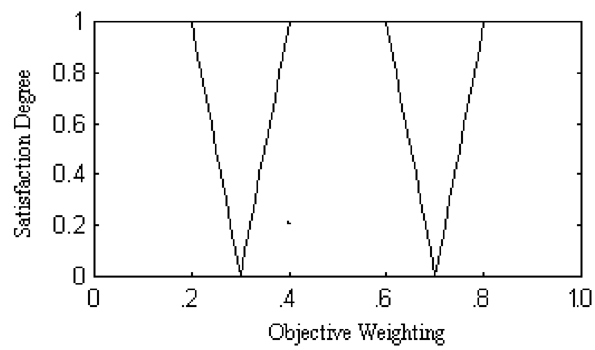

Fig. 3: Linguist variable for the weight of an objective

The difficulty with multi-objective problems is to express the relevance of each objective through numeric values and to get the best results. Using the linguistics variables [11], a better tolerance in the weight setting for conflict solution process. The new objective function, called *decision fuzzy function* or $\widetilde{F}(X)$ set, can be written:

$$\widetilde{F}(X) = \widetilde{W}_{g1}\mu_{g1}(X) + \widetilde{W}_{g2}\mu_{g2}(X) + \sum_{i=3}^{m+2}\widetilde{W}_{gi}\mu_{gi}(X) + \sum_{j=3}^{m+4}\widetilde{W}_{gj}\mu_{gj}(X) \quad (16)$$

The $\widetilde{F}(X)$ set has $m+4$ membership function corresponding to the 2 objectives (Z_1 e Z_2) and to the m+2 constraints of the problem (8)-(10). The coefficient $\widetilde{W}_i$ is the weight of the objective i, $\mu_{gi}(X)$ is the degree of membership or satisfaction of the objective i e $X = [x_1, x_2, \ldots, x_n]^T$ is the vector of the n control or decision variables.

The formulation and resolution of non-linear problems follows the same principal used for linear ones: the objectives and constraints are transformed into fuzzy sets described by membership functions weighted by linguistic terms.

3.2 Formulation of the Problem

The Optimal Reactive Power Flow problem can be formulated as

$$Minimize \;\; F(u,x) \qquad (17)$$

subject to

$$g_i(u,x) = 0 \qquad (18)$$

$$h_i(u,x) \leq 0 \qquad (19)$$

for i = 0, … , N_C, where N_C is the number of contingency cases and the index zero represents the base case for the intact system. In this formulation (17) can be written as

$$F(u,x) = \sum_{i=1}^{N_C} \sum_{j=1}^{N} (V_j - V_j^*)^2 \qquad (20)$$

where, N is the number of busses, V_j the module of the actual voltage and V_j^* the optimum value of the voltage magnitude at bus j in the intact system. The vector functions $g_i(u, x)$ are the load flow equations and $h_i(u, x)$ are the constraints of the system. In this work the problem (17)-(19) is formulated considering only the base case (i = 0). The objective is eliminate voltage violations, minimize the control actions by rescheduling the voltage and reactive power control variables and maximize the VCM supplied by ANN. The objectives functions, witch form the Decision Fuzzy Function (DFF), are voltage magnitude at load buses, reactive power output of generators, voltage magnitude at generator buses, transformer taps and the VCM of weakest bus bar.

The functions for describing the degree of membership of the voltage magnitudes at generator buses are described by

$$\mu_{gi} = \begin{cases} 1 & for \;\; V_i^{\min} \leq V_i \leq V_i^{\max} \\ exp\left(\dfrac{-(V_i - V_i^{\min})^2}{2\sigma^2}\right) & for \;\; V_i < V_i^{\min} \\ exp\left(\dfrac{-(V_i - V_i^{\max})^2}{2\sigma^2}\right) & for \;\; V_i > V_i^{\max} \end{cases} \qquad (21)$$

for $i \in N_G$, where V_i is the actual voltage magnitude at bus i, $V_i^{\min}$ and $V_i^{\max}$ are minimum and maximum operating limits. Figure 4 presents the membership function that describes the fuzzy sets of the voltage magnitudes at generator buses.

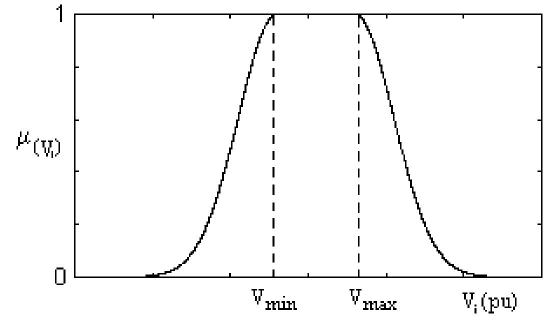

Fig. 4: Fuzzy set of voltage magnitude at generators

The functions which describe the membership degree for transformer taps and reactive power sources output are of the same kind of those for the voltage magnitude, with the variable t for the tap, and Q for the reactive power sources replacing the variable V in the pertinent equations.

The voltage magnitude at load buses are described by

$$\mu_{gk} = \begin{cases} 1 & for \;\; V_k = V_k^d \\ exp\left(\dfrac{-(V_k - V_k^d)^2}{2\sigma^2}\right) & otherwise \end{cases} \qquad (22)$$

for $k \in N_{BC}$, where V_k is the actual voltage magnitude at bus k and V_k^d is the target voltage magnitude. Figure 5 shows the functions for the fuzzy sets for the voltage magnitude at load bus.

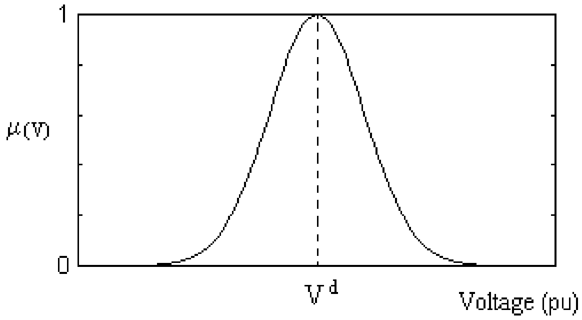

Fig. 5: F*uzzy set* for voltage magnitude at load buses

In Figure 5, if the voltage magnitude leaves V^d, towards the limits its degree of membership tends to zero.

The function which present the membership degree of VCM is describe by:

$$\mu(\Delta Q) = \frac{1}{1 + e^{-k(\Delta Q - C)}} \qquad (23)$$

where ΔQ is the actual VCM, C is the coefficient which determine the distance of the function $\mu(\Delta Q)$ with respect to vertical axis and the k is the coefficient which determine the inclination of the $\mu(\Delta Q)$ in C. Figure 6 shows the membership functions for the voltage collapse margin at the weakest load bus.

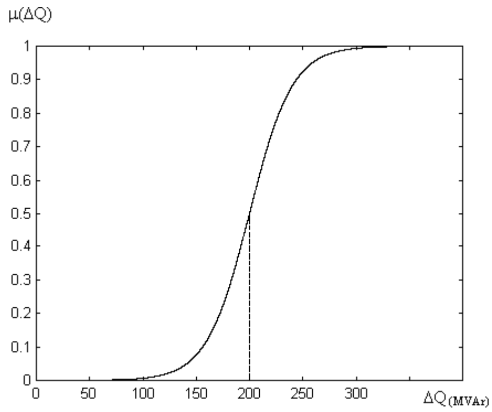

Fig. 6: Fuzzy set of voltage collapse margin

3.3 Dynamic Smooth Weighting of the Objectives

The determination of the weights is dynamic; therefore, an objective can have different values for the weight during the iterative process. If the voltage magnitude is out of the limits its membership function has a high weight; however, the weight decreases as the voltage magnitude gets close to the desired value. For instance, for an output of reactive power of generators within its bounds the weight is low, but it is high for a reactive power output out of bounds. Table 1 shows the weights for the voltage magnitudes.

Table 1: Linguistic weights for voltage magnitudes

Range	Linguistic weight
$\left\lvert V_i - V_i^d \right\rvert \le 0.1$	"low weight"
$0.1 < \left\lvert V_i - V_i^d \right\rvert < 0.2$	"mean weight"
$\left\lvert V_i - V_i^d \right\rvert \ge 0.2$	"high weight"

The same rules of Table 1 applies for transformer taps, only replacing V_i and V_i^d by T_i e T_i^d.

The fuzzy sets, which represent the linguist weights for the objectives, are trapezoidal functions. Table 2 shows the relation between the weights and the respective trapeze vertex.

Table 2: Vertex of fuzzy sets for linguist weight

Linguistic weight	Trapeze vertex
"low weight"	[0.0, 0.03, 0.07, 1.0]
"*mean weight*"	[0.1, 0.23, 0.37, 0.5]
"high weight"	[0.5, 0.63, 0.87, 1.0]

The closer to its limits the objective function value, the higher the value of its weight in relation to the set $\widetilde{F}(u,x)$.

3.4 The Fuzzy Set of Decision

The formulation of the problem assumes a power system out of the operating limits. Thus, the objective is to maximize the decision fuzzy set $\widetilde{F}(u,x)$, described by

$$\widetilde{F}(u,x) = \widetilde{W}\mu(\Delta Q) + \sum_i \widetilde{W}_i \mu_i(V_i) + \\ + \sum_j \widetilde{W}_j \mu_j(T_j) + \sum_k \widetilde{W}_k \mu_k(V_k) + \sum_l \widetilde{W}_l \mu_l(Q_l) \qquad (24)$$

for $i, l \in N_G$, $j \in N_T$ and $k \in N_{BC}$.

The same approach adopted for the optimization of the base case intact system can be used for the optimization of all contingencies. The difference being the value of the desired voltage magnitude at load buses which should be set to the value of the voltage magnitude of the base case. This formulation is useful in the planning stage when all anticipated or the worst case contingencies are to be investigated.

3.5 Maximization of the Fuzzy Set of Decision

A steepest acclivity gradient search is adopted to optimize the set $\widetilde{F}(u,x)$. The termination criterion is presence of violations; thereby, the algorithm is said to converge when all violation are eliminated. Thus, the search can stop far away from the maximum value of $\widetilde{F}(u,x)$. Other termination criteria can be see in [12].

Considering which the membership functions and its independent variable vary directly only in relationship the control variable, the gradient of the fuzzy set $\widetilde{F}(u,x)$ can be express as

$$\nabla_u \widetilde{F}(u,x) = \left[\frac{\partial \widetilde{F}}{\partial u_1}, \cdots, \frac{\partial \widetilde{F}}{\partial u_p}, \frac{\partial \widetilde{F}}{\partial u_{p+1}}, \cdots, \frac{\partial \widetilde{F}}{\partial u_n} \right]^T \quad (25)$$

where n is the number of control variable. The change of fuzzy set $\widetilde{F}(u,x)$ with respect to *p-th* control variable result in

$$\frac{\partial \widetilde{F}(u,x)}{\partial u_p} = \frac{\partial}{\partial u_p} \Big[\widetilde{W} \mu(\Delta Q) + \sum_i \widetilde{W}_i \mu_i(V_i) + \\ + \sum_j \widetilde{W}_j \mu_j(T_j) + \sum_k \widetilde{W}_k \mu_k(V_k) + \sum_l \widetilde{W}_l \mu_l(V_l) \Big] \quad (26)$$

for i e $l \in N_G$, $j \in N_T$ e $k \in N_{BC}$.

The fuzzy weights does not vary directly in function of control elements, but in agreement with Table 1. Thereby, these weights are constants to compute of gradient vector and the equation (26) can be express as

$$\frac{\partial \widetilde{F}(u,x)}{\partial u_p} = \widetilde{W} \frac{\partial \mu(\Delta Q)}{\partial u_p} + \sum_i \widetilde{W}_i \frac{\partial \mu_i(V_i)}{\partial u_p} + \\ + \sum_j \widetilde{W}_j \frac{\partial \mu_j(T_j)}{\partial u_p} + \sum_k \widetilde{W}_k \frac{\partial \mu_k(V_k)}{\partial u_p} + \\ + \sum_l \widetilde{W}_l \frac{\partial \mu_l(Q_l)}{\partial u_p} \quad (27)$$

for i and $l \in N_G$, $j \in N_T$ and $k \in N_{BC}$..

The function $\mu(\Delta Q)$ is similar with $\mu(Y)$, because the collapse voltage margin is supply by ANN output Y. The partial derivation $\partial\mu(Y)/\partial u_p$ can be resulted using chain role, as follow

$$\frac{\partial \mu(Y)}{\partial u_p} = \frac{\partial \mu(Y)}{\partial Y} \frac{\partial Y}{\partial u_p} \quad (28)$$

For solve Equation (28), include the ANN topology in the problem is necessary. Normally, this is not made because after training the ANN is considering as black box that supply generalization results. The derivation $\partial\mu_l/\partial Y$ is direct, because the membership function μ vary directly with respect to Y. Nevertheless, find the derivation $\partial Y/\partial u_p$ is necessary considering the ANN mathematical model presented in Item 2. In this case, the variation of output Y with respect to control element u_p is not direct, because $Y = f(v)$. The development of this derivation, for tree layers ANN, is present in [13]. The final equation result in

$$\frac{\partial Y}{\partial u_p} = f'(v) \sum_{i=1}^{m} w_i f'(v_i^{(1)}) w_{ip}^{(1)} \quad (29)$$

where W_i the *i-th* synaptic weight of the output neuron Y and W_{ip} is the *p-th* synaptic weight of output neuron $Y_i^{(1)} = f(v_i^{(1)})$. The subscript 1 indicate the layer one, that is, the first hidden layer where the neuron i is localized.

Considering which the *p-th* control variable does not change the membership function of other control variable, the second and third sum of equation (27) results in

$$\sum_i \widetilde{W}_i \frac{\partial \mu_i(V_i)}{\partial u_p} + \\ + \sum_j \widetilde{W}_j \frac{\partial \mu_j(T_j)}{\partial u_p} \begin{cases} = 0 & for\ i \neq p \\ & or\ j \neq p \\ = \dfrac{\partial \mu_p(u_p)}{\partial u_p} & for\ i = p \\ & or\ j = p \end{cases} \quad (30)$$

The fourth sum of equation (27), which correspond the derivation of membership function μ_k with respect to control variable u_p, is given by chain role as follows

$$\frac{\partial \mu_k(V_k)}{\partial u_p} = \frac{\partial \mu_i(V_k)}{\partial V_k} \frac{\partial V_k}{\partial u_p} \quad (31)$$

where the first term is a derivation of equation (21) and the second term is the derivation of the state variable k with respect to a control variable p, which correspond, in power system, a S_{kp} element of the sensitivity matrix. Thereby, the equation (31) can be wrote as

$$\frac{\partial\mu_k(V_k)}{\partial u_p} = \frac{\partial\mu_i(V_k)}{\partial V_k} S_{kp}^{ini} \qquad (32)$$

where S_{kp}^{ini} the element of sensitivity matrix for initial state.

The last sum of equation (27) is given by a chain role too, resulting

$$\frac{\partial\mu_l(Q_l)}{\partial u_p} = \frac{\partial\mu_i(Q_l)}{\partial Q_l} \frac{\partial Q_l}{\partial u_p} \qquad (33)$$

where the first term is the derivation of equation (22), when the variable *Q* for the reactive power sources replacing the variable *V* in the pertinent equations, and the second term is a instantaneous variation of reactive power dispatch Q_l with respect a control variable u_p. Considering the load in the *l* bus constant, the term $\partial Q_l / \partial u_p$ is the J_{lp} element of *Jacobian* matrix. Thus, the equation (33) can be wrote as

$$\frac{\partial\mu_l(Q_l)}{\partial u_p} = \frac{\partial\mu_i(Q_l)}{\partial Q_l} J_{lp}^{ini} \qquad (34)$$

where J_{lp}^{ini} is the element of *Jacobean* matrix in initial state.

Substituting equations (29), (30), (32) and (34) in (27), the *p-th* element of gradient vector of $\widetilde{F}(u,x)$ results in

$$\frac{\partial\widetilde{F}(u,x)}{\partial u_p} = \frac{\partial\mu(Y)}{\partial Y}\frac{\partial Y}{\partial u_p} + \widetilde{W}_p\frac{\partial\mu_p(u_p)}{\partial u_p} + \sum_k \widetilde{W}_k \frac{\partial\mu_k(V_k)}{\partial V_k} S_{kp}^{ini} + \sum_l \widetilde{W}_l \frac{\partial\mu_l(Q_l)}{\partial Q_l} J_{lp}^{ini} \qquad (35)$$

for $j \in N_T$ e $k \in N_{BC}$..

The centroid tech for result a numerical gradient vector is used for each fuzzy set in Equation (35).

3.6 Control Variables Adjustment

The control variables adjustments are calculated in function of the length of η step on $\widetilde{F}(u,x)$ surface. In the iteration *t+1*, the adjustment of the control variable *p* is

$$u_p^{(t+1)} = \begin{cases} u_p^{\min} & for \;\; u_p^{(t)} + \eta\nabla F_p^{(t)} < u_p^{\min} \\ u_p^{\max} & for \;\; u_p^{(t)} + \eta\nabla F_p^{(t)} > u_p^{\max} \\ u_p^{(t)} + \eta\nabla F_p^{(t)} & otherwise \end{cases} \qquad (36)$$

The length of the η step in direction of the gradient has fundamental importance in an iterative process. Using an allegory step length, a number of iterations can be made a lot above of necessary or not obtain convergence. There are possibilities that minimize the problem, as maximize the η step to each iteration, finding great values inside of the permissible limits [14]. Other possibility that minimize the problem is to use, for each iteration, the η step equal the Euclidean distance or Euclidean norm between the current and desired voltage. However, using a step that varies with the distance Euclidean in the $\widetilde{F}(u,x)$ surface, exist a portion of this distance that provides better acting. Thereby, the step on the $\widetilde{F}(u,x)$ surface can be defined as

$$\eta^{(t)} = \alpha \cdot \left\| X^{(t)} - X^d \right\| \qquad (37)$$

where α a portion of the Euclidean distance on *t* iteration.

This algorithm can be summary following steps:

(i) Perform the load flow, by *E&PSG 4.01* program [14], and compute sensitivity and *Jacobean* matrix;
(ii) Compute fuzzy weight of the objectives;
(iii) Compute the $\widetilde{F}(u,x)$ set;
(iv) Compute gradient vector of the $\widetilde{F}(u,x)$;
(v) Compute the Euclidean distance;
(vi) Adjust the control variable, using the gradient vector, and state variable, using the sensitivity matrix;
(vii) Verify the existence of violations. For the positive case, the processes is finished. Otherwise, back to (ii) step.

4 Numerical Results

The method was programmed integrating a Matlab 4.2c.1, SiNe 3.0 - Neural Simulator and E&PSG 4.01 program on a AMD 586 133 MHz processor. Several case studies were investigated using the IEEE-30 bus test systems. The *n-1* criterion was adopted and the lower and the upper bus voltage limits were set at 0.975 and 1.025 pu, with tolerance of 0.05 pu on the lower limits for contingency cases. The 30-bus was regarded as the weakest bus. The fuzzy set $\widetilde{F}(u,x)$ had one VCM membership function, 30 state variable membership function and 10 control variable membership function. The ANN training data was made varying all generation buses randomly; thus, VCM and load bus voltage was changed. The used ANN has six outputs, nine hidden neurons and one output neuron. The global error was 4.54 x 10^{-4} and 18.89 x 10^{-4} in the training and testing phase, respectively.

The control actions through the transformer taps are eliminated; only voltage of control bus are directly controlled. In the initial state, all control bus are fixed in 1 pu.

A systematic analysis for three simulations, beginning in same point, was performed. The difference between three simulations was the weight of VCM membership function, which show the VCM enhancement and monitoring total active power loss. Table 3 show the results after optimization process.

Table 3: Optimization of IEEE-30 bus network

	Initial State	W_{low}	W_{mean}	W_{high}
Loss (MW)	3.66	3.83	4.49	4.88
Loss (MVAr)	3.17	2.88	5.49	6.96
Least Reserve (MVAr)	43 %	39 %	34 %	16 %
Least Voltage (pu)*	0.7857	0.8186	0.8078	0.8137
No. of Violations*	19	5	5	5
No. of Iterations	—	2	3	4

* considering all contingencies

Considering Table 3 indicator, the first simulation (W_{low}) obtained the best results with respect to losses, because the VCM had few relevance. The VCM of 30-bus increase when its relevance grow up; nevertheless, total active power loss and reactive power reserve increase. This evidence corresponds the need to increase the reactive power generation to increase VCM.

Figure 7 show VCM of 30-bus for each iteration in three simulations.

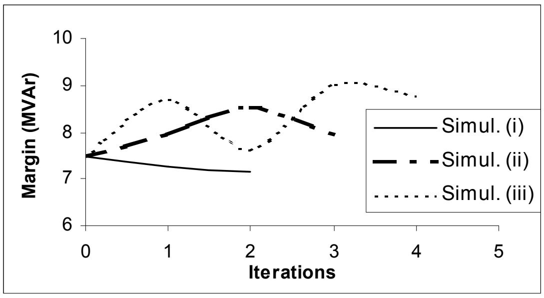

Fig. 7: Voltage Collapse Margin per Iteration

In first simulation (W_{low}), the VCM decrease each iteration and have bad result than others simulations, because it low weight. In others two simulations (W_{mean} and W_{high}), the VCM varying in optimization process, because it has mean and high relevance, resulting conflicts between objectives. Specifically in third simulation, can be see a tendency in increase VCM much more, because the high membership function weight.

The Pareto solution, where each one of n-objective is a coordinate axis in the $\Re^n$ space, is other important analysis. Each point, in the same Pareto solution, is a system state. The simulations set forms a trajectory in the state space. For the IEEE-30 bus system, two objectives are regarded in the Pareto Solution, the VCM of 30-bus and the total active power loss. The optimum point of control variable and ANN weight result the coordinate (∞, 0) in the Figure 8; nevertheless, in practical it is impossible. With this analysis, the total active power loss monitoring is possible. Thus, it is possible to check if the coasts for increase security margin is admissible.

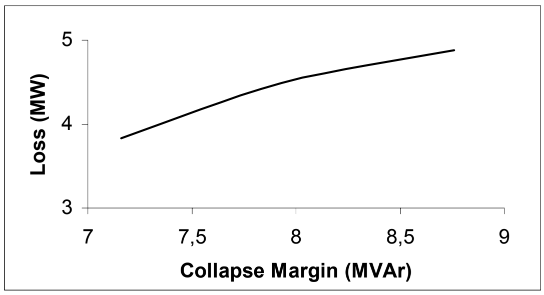

Fig. 8: Pareto Solution: Loss x VCM

The results of the investigations have been promising, with the smooth satisfaction of all the objectives, that is, elimination of all violations and setting of all control variables and output of generators close to their middle range limits. The results have shown the ability of the method in assuring good reserve capabilities of the network. Work is under way to include the objective of the enforcement of voltage collapse margins for a set of pilot buses. Also, a grade code for larger networks is under development, with the implementation of the algorithm as an extension of the EPSG 4.01 program.

5 Acknowledgments

Maury M. Gouvêa Jr. gratefully acknowledges the financial support for this project provided by FAPEMIG - Fundação de Amparo à Pesquisa do Estado de Minas Gerais, Brazil.

6 Conclusion

This work presented a new methodology that integrates the fuzzy set technology with the sensibility analysis for formulation and resolution of the optimal reactive power flow problem. In this approach, all objectives and constraints are treated by satisfaction degree weighted by linguistic terms, which present the advantage of including, in the same objection function, distinct and conflicting objectives.

Additionally, the ANN was used to supply voltage collapse margin of the weakest bus bar. This voltage collapse margin, supplied by ANN, is also included in objective function and weighted by linguistic terms. The advantage of this approach is to use ANN architecture in sensibility analysis. The voltage collapse variation with respect to the control variables is given by ANN architecture. Thus, the necessity of the knowledge of the voltage collapse margin formula is eliminated.

The implanted algorithm was tested in IEEE-14 and IEEE-30 bus bar system, eliminating all violations and improving the reactive power reserve of the generator. This is an important result, because the control elements were adjusted without affecting the security margin of the system.

Reference:

[1] Y. Y. Haimes, K. Tarvainen, T. Shima, J. Thadathil, *Hierarchical Multiobjective Analysis of Large-Scale Systems*, Henisphere Publishing Corporation, 1989.

[2] L. A. Zadeh, Fuzzy Logic, *IEEE Computer*, 1988, pp. 83-92.

[3] S. U. Mohandas, T. A. Phelps, K. M. Ragsdell, Structural Optimization Using a Fuzzy Goal Programming Approach, *Computer and Structures*, Vol. 37, No. 1, 1990, pp. 1-8.

[4] V. C. Ramesh, X. Li, A Fuzzy Multiobjective Approach to Contingency Constrained OPF, *IEEE Transactions on Power Systems*, Vol. 12, No. 3, 1997, pp. 1348-1354.

[5] *IEEE Technology Update Series: Neural Networks Applications*, IEEE Technical Activities Board, New York City (NY), 1996.

[6] R. Atteri, M. A. El-Sharkawi, Static Security Assessment of Power System Using Kohonem Neural Network, *IEEE Technology Update Series: Neural Networks Applications*, 1996, pp. 297-301.

[7] H. Kanoh, K. Kanemaru, M. Kaneta, M. Nishiura, A Study on Pratical Fault Location for Power Transmission Lines Using Neural Networks, *IEEE Technology Update Series: Neural Networks Applications*, 1996, pp. 245-249.

[8] B. S. Kermanshahi, C. H. Poskar, G. Swift, W. Buhr, A. Silk, Artificial Neural Network for Forecasting Daily Loads of a Canadian Electric Utility, *IEEE Technology Update Series: Neural Networks Applications*, 1996, pp. 268-273.

[9] F. Rosenblatt, The Perceptron: A probabilistic model for information storage and organization in the brain, *Psychological Review*, Vol. 65, 1958, pp. 386-408.

[10] D. Rumelhart, G. Hinton, R. Williams, Learning Internal Representations by Error Propagation, In D. E. Rumelhart and J. L. McClelland (Editors), *Parallel Distributed Processing: Explorations in the Microstructure of Cognition*, MIT Press, Cambridge (MA), 1986.

[11] L. A. Zadeh, Knowledge Representation in Fuzzy Logic, *IEEE Transactions on Knowledge and Data Engineering*, Vol. 1, No. 1, 1989, pp. 89-100.

[12] C. Ejebe, G. D. Irisarri, S. Mokhtari, O. Obadina, P. Ristanovic, J. Tong, Methods for Contingency Screening and Ranking for Voltage Stability Analysis of Power Systems, *IEEE Transactions on Power Systems*, Vol. 11, No. 1, 1996.

[13] M. M. Gouvêa Jr., *Sistema Híbrido Neuro-Fuzzy Aplicado ao Problema do Fluxo Ótimo de Potência Reativa*, Master Thesis, Pontifical Catholic University of Minas Gerais, Brazil, 1998.

[14] L. D. B. Terra, M. J. Short, Security-Constrained Reactive Power Dispatch, *IEEE Transactions on Power Systems*, Vol. 6, No. 1, 1991, pp. 109-117.